

SAW NDE TECHNIQUES FOR MONITORING THE GROWTH BEHAVIOR OF SMALL
SURFACE FATIGUE CRACKS

M. T. Resch[†], B. D. London[†], G. F. Ramusat*,
H. H. Yuce^{††}, D. V. Nelson^{††} and J. C. Shyne[†]

Stanford University, Stanford, California 94305 USA

[†] Department of Materials Science and Engineering

^{††} Department of Mechanical Engineering

* Visiting Scholar, O.N.E.R.A., France

INTRODUCTION

Recent experiments have demonstrated that surface acoustic waves (SAW), or Rayleigh waves, can be used to predict the size and normalized stress intensity factor of small surface fatigue cracks. In particular, SAW methods have been able to monitor the growth of small surface fatigue cracks during the early stages of crack propagation in 7075-T651 aluminum, quenched and tempered martensitic 4340 steel, and to predict the fracture stress of Pyrex glass containing small surface cracks. The SAW technique has considerable promise as a new research tool for the study of the early stages of fatigue, and it has important implications for the practical non-destructive evaluation of components made of ceramics and metals.

Briefly stated, the SAW technique consists of measuring the reflection coefficient of Rayleigh waves from an isolated surface crack. The method uses SAW wedge transducers to produce the Rayleigh waves and to receive the reflected signals. Physically, the reflection coefficient is the ratio of the maximum amplitude of the reflected signal from the crack picked up by the receiving transducer to the maximum amplitude of the signal input to the sending transducer. A surface crack is illuminated with a tone burst of several wavelengths duration from one transducer, and the reflected echo received at the other transducer. In the next section, theory^{1,2} is summarized which shows how the reflection coefficient of Rayleigh waves can be used to infer the maximum normalized stress intensity factor and depth of a surface crack.

VERIFICATION AND PRACTICAL LIMITATIONS OF THE SCATTERING THEORY

Crack Depth Prediction

Resch et al.³⁻⁵ have shown that the maximum crack depth, a , of a surface crack can be evaluated by acoustically measuring the SAW reflection coefficient from a crack and optically measuring the length, $2c$, of the intersection of the crack with the free surface. The cracks are assumed to be flat, with semi-elliptical shape such that the crack aspect ratio, a/c , is less than unity. Additionally, the wavelength normalized crack depth, κa , (where $\kappa = 2\pi/\lambda$) must be less than unity to ensure that the long wavelength conditions are maintained. Under these conditions,

$$S_{21} = \frac{2\pi f_z \eta c a^2 \kappa^2}{3(1-\nu)w\phi} [B_0 + B_1(\kappa a) + B_2(\kappa a)^2] \quad (1)$$

The parameters in Equation 1 are defined in Refs. 3-5.

Maximum Normalized Stress Intensity Factor

The maximum normalized stress intensity factor of a crack, $k_{I\max}$, is defined as the maximum mode I stress intensity factor divided by the applied stress, σ_{zz} , that is,

$$k_{I\max} = \frac{K_{I\max}}{\sigma_{zz}} \quad (2)$$

Resch et al.^{6,7} have shown that $k_{I\max}$ may be evaluated by measuring the reflection coefficient of a SAW incident on a surface crack, that is,

$$k_{I\max} = \gamma \left[\frac{3EV_R^2 w S_{21}}{(1-\nu^2)\pi^3 \omega^2 V_S^2 \rho f_z \eta [1-(V_S/V_L)^2]^2} \right]^{1/6} \quad (3)$$

The parameters in Equation 3 are defined in Ref. 6,7.

Comparison of Acoustic Predictions vs. Post-Fracture Measurements of Size.

Measurements of the reflection coefficient from small surface cracks in Pyrex glass and 7075-T651 aluminum have been reported

previously in the literature³⁻⁷. In these experiments a Knoop microhardness indenter was used to produce small surface cracks in specimens of Pyrex glass. In 7075-T651 aluminum an infrared pulsed YAG laser was used to produce nucleation sites for small surface fatigue cracks, while in martensitic 4340 steel the spark discharge from a battery charger was used to produce nucleation sites. The crack size which existed during SAW scattering measurements in Pyrex specimens was obtained using optical microscopy to observe the deformation pattern around the periphery of the surface crack caused by the Knoop indenter. Crack size was verified in 7075-T651 aluminum by using variable amplitude loading to mark intermediate crack contours with specific deformation textures which could be observed post-fracture in an SEM. In 4340 steel, crack size was ascertained by deliberate formation of an oxide layer formed during tempering at 300°C for 2-3 hours. After tempering, the specimen was cycled to failure and the oxide layer measured either optically or with a scanning electron microscope.

Each measurement of the reflection coefficient combined with an optical measurement of the crack length at the surface makes it possible to obtain the corresponding acoustic prediction of crack depth, a_p , utilizing Equation 1. It has been observed experimentally that the amplitude of the reflection coefficient from a crack is only useful for making depth predictions when the measurement is made with a tensile stress applied to the specimen large enough to cause the adjacent crack faces of the surface crack to separate. Figure 1 shows schematically how the reflection coefficient varies with applied stress evaluated in the vicinity of the crack. The reflection coefficient, S_{21} , "saturates" at a characteristic value of the applied stress denoted σ_{sat} . For applied stress $\sigma > \sigma_{sat}$, the reflection coefficient does not increase with increasing applied stress up to the yield stress of the material. All acoustic predictions of crack depth are made with S_{21} measured at the particular value of σ_{sat} which exists during the scattering measurement. In addition to static measurements of σ_{sat} , it has been observed experimentally that the value of σ_{sat} changes during the growth of a crack as a function of stress history, as will be described later.

Experimental Uncertainty

Kline and McClintock⁸ have shown that the uncertainty w_R , of a variable with magnitude $V_i = (V_i - w_i < V_i < V_i + w_i)$ can be calculated from the expression

$$w_R = \left[\left(\frac{\partial R}{\partial V_i} w_i \right)^2 \right]^{1/2} \quad (4)$$

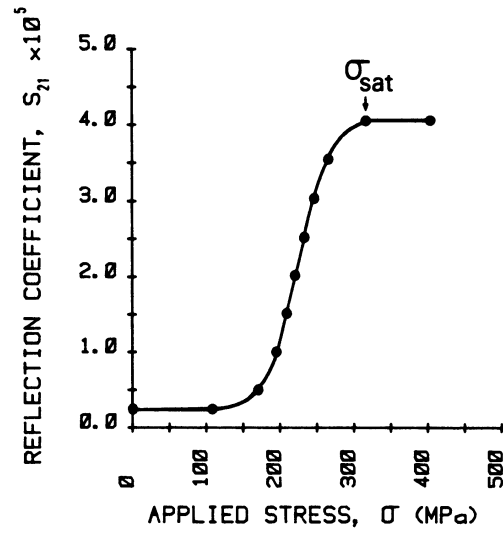


Figure 1. Schematic of opening behavior of a small surface crack.

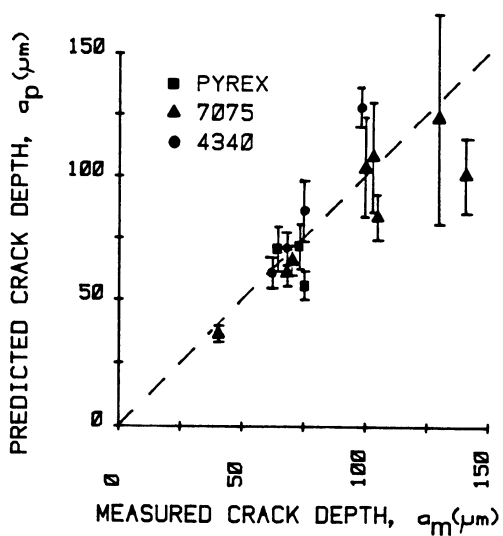


Figure 2. Acoustic prediction of crack depth vs. measured crack depth with estimation of experimental uncertainty for cracks with a/c ratios between 0.3 and 1.

In the present case, eleven independent variables are used in Equation 4 to correlate crack depth with experimental observations of SAW reflection measurements. The variables are: Poisson's ratio, ν , Young's modulus, E , the mass density, ρ , the acoustic wave frequency, f , the scattering angle, ϕ , the distance from the crack to the transducers, z , the transducer insertion loss, η_T , the receiving amplifier gain, η_A , the zero-to-peak amplitude of the signal input to transducer 1, V_1 , half the crack length at the surface, c , and the amplified crack reflection amplitude, V_2^m .

In Fig. 2 the experimental uncertainty of each prediction of crack depth is denoted by error bars. The uncertainty increases with crack size because of the increase in slope $\partial a / \partial V_2^m$ with increasing values of a . The agreement between predictions and observations is reasonably good, particularly in view of the uncertainties involved.

USES OF THE SAW TECHNIQUE

A Fatigue Experiment

Consider the following fatigue experiment which demonstrates the previously described techniques. A small surface crack was introduced in a specimen of 4340 steel in the quenched (martensitic) condition by a spark discharge. After the crack was grown to a size above which the reflection was readily discernable, the damaged region was removed by careful surface grinding with final surface removal rate of 1/2 mil (12.5 μm) per pass, until the signal was just discernable above the noise level. The specimen was then tempered at 300°C for two hours to mark the depth of the precrack. After tempering, the specimen was subjected to the loading sequence shown in Fig. 3a. The reflection coefficient, S_{21} , was measured at intervals during the fatigue cycling. The stress at saturation, σ_{sat} , was measured at the beginning of each constant amplitude interval. The simplifying assumption of $a=c$ was made for this test.

Each measurement of the reflection coefficient was then used to calculate the depth of the assumed half penny shaped crack using Equation 1. In Fig. 3b. these values of crack depth are plotted versus the number of cycles, N . The maximum normalized stress intensity factor, $K_{I\text{max}}$, for the crack was calculated using Equation 2 at each value of S_{21} . Noting that the maximum stress intensity factor, $K_{I\text{max}}$, is simply $\sigma K_{I\text{max}}$, the data can be combined to calculate the stress intensity factor range $\Delta K_{I\text{max}} = K_{I\text{max}} (\sigma_{\text{max}} - \sigma_{\text{min}})$ during the fatigue experiment. In Fig. 3c. these values of $\Delta K_{I\text{max}}$ allow comparisons of growth rate of small cracks with that of large cracks of the same material. We do not imply, however, that ΔK_I is necessarily the proper parameter for correlating small crack growth behavior.

It was noted previously that measurements of σ_{sat} were per-

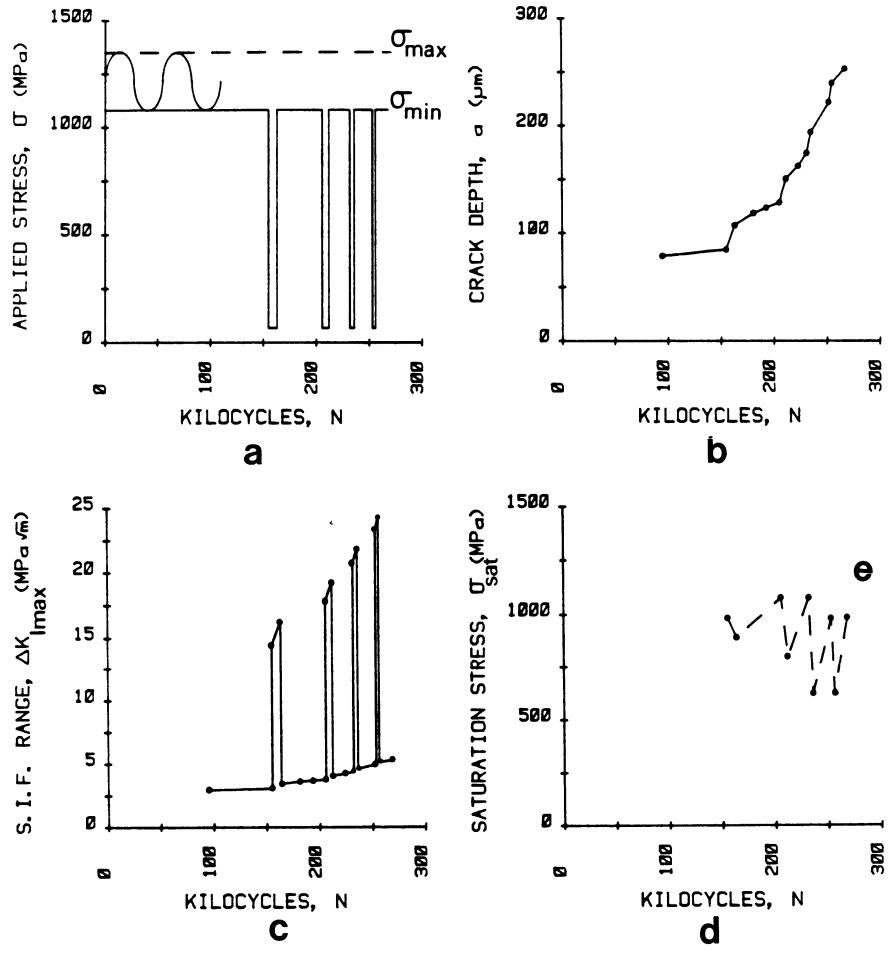


Figure 3. (a) Stress history (b) Crack depth history (c) Stress intensity factor range history (d) Opening history.

formed in conjunction with measurements of S_{21} . During the fatigue test the magnitude of σ_{sat} was found to change substantially with changes in the load ratio, R . Measured values of σ_{sat} are plotted versus N in Fig. 3d. In this experiment, the saturation stress was only measured at the beginning of each interval of constant R . It is not currently known how σ_{sat} changes during constant amplitude loading as a function of previous applied stress history. The dashed lines between data points evaluated from this experiment merely demonstrate the trend that cycling at $R=0.8$ followed by $R=0.05$ caused σ_{sat} to become smaller, and that cycling at $R=0.8$ after $R=0.05$ caused σ_{sat} to increase substantially.

This preliminary experiment shows the potential of the SAW technique to monitor σ_{sat} . Future experiments are planned to investigate more rigorously the variation of σ_{sat} with crack growth and loading conditions.

SAW-SEM Studies of Opening Behavior

Another preliminary experiment has been performed in order to investigate the relationship (if any) between the optically determined crack closure stress, σ_{c1} , and the stress at which saturation of the SAW reflection coefficient occurs, σ_{sat} . Small specimens have been designed which facilitate the measurement of CMOD and CTOD with the specimen under load in an SEM chamber, yet are large enough to accommodate two SAW wedge transducers for reflection coefficient measurements in-situ during a fatigue experiment in the MTS testing machine.

Specimens are prepared for combined SAW/SEM analysis by first attaching a strain gage on the side of the specimen opposite from the crack. Measurements of the SAW reflection coefficient are made in an MTS testing machine with the specimen in cantilevered bending, by adjusting the specimen deflection to give the desired strain levels. A typical measurement of the SAW reflection coefficient versus stress is shown in Fig. 4a. The specimen is then removed from the testing machine and attached to the SEM flexure jig. At each value of the strain at which the reflection coefficient was measured, the CMOD is measured in a SEM at a magnification of approximately 10,000X. CMOD measurements versus stress for the specimen behavior described in Fig. 4a. are shown in Fig. 4b. In this experiment, σ_{c1} was determined to be 100 MPa, while the stress at which saturation occurs for the reflection coefficient, σ_{sat} , was found to be 350 MPa. These preliminary results provide encouragement that σ_{c1} and σ_{sat} may be related. More experiments are planned to obtain additional data to investigate the possible correspondence of SAW and SEM measurements.

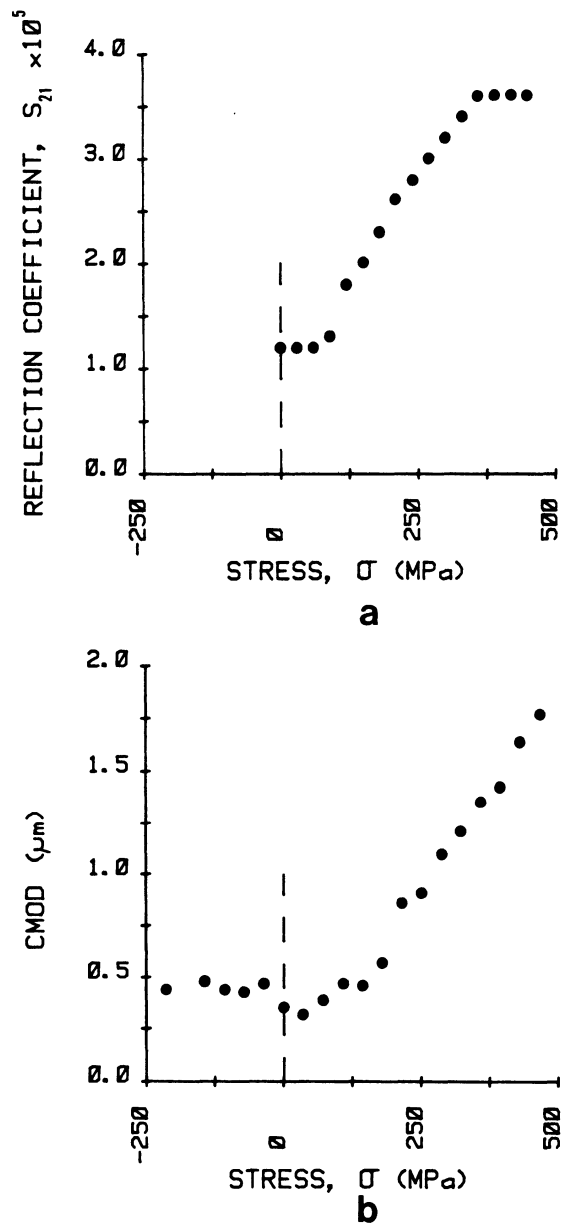


Figure 4. Opening behavior of small surface fatigue crack in 7075-T651 aluminum showing (a) S_{21} vs. σ , and (b) CMOD vs. σ .

DISCUSSION

Current SAW NDE technology has made it possible to obtain a great deal of information during fatigue experiments about the growth of small surface cracks. Changes in crack shape below the surface can be detected, as well as changes in crack opening behavior. One obvious limitation of the technique occurs during non-uniform crack growth around the periphery of the advancing fatigue crack. Morris et al⁹⁻¹⁰ have demonstrated that microstructural features such as grain boundaries and inclusions dominate micro-crack growth kinetics, producing uneven crack growth rate at each crack tip which depends on the proximity of the tips to grain boundaries. This type of behavior observed at the surface is also expected at points along the crack edge below the surface. As a result, the assumption of a semi-elliptical crack shape below the surface can only be viewed as a reasonably good approximation. Also, the SAW determination of opening stress is an "averaged" value for a crack. Future studies are planned which will carefully monitor opening stress determined from crack center CMOD and crack tip CTOD measurements for comparison with opening stress determined by the SAW technique, as a function of crack growth. Knowledge of how opening stress varies with growth should be helpful in interpreting the growth behavior of small cracks.

Another topic of great concern in SAW NDE measurements concerns the interpretation of the observed crack opening behavior of small surface cracks. It is not currently known how the distribution of contact points on adjacent crack faces changes during loading and unloading of a body containing residual stresses in the vicinity of the crack. The complexity of the situation is compounded by the effects of oxide-induced, and deformation induced crack closure, which can affect the opening behavior of small growing fatigue cracks. The redeeming value of SAW measurements of opening behavior for real surface fatigue cracks is that the portion of the applied stress cycles where the crack is completely open is easily measured during the test. Additionally, cycling at a stress from zero to somewhat below the saturation stress produces a calculated range of the stress intensity factor which corresponds roughly to the threshold value of ΔK as measured from large fatigue cracks for the alloys studied thus far. It is hoped that a greater understanding of the physical processes occurring around the crack edge during the application of cyclic stresses below the saturation stress will lead to the understanding of the effect of the stress ratio on the growth rate of small surface fatigue cracks and shed some light on the existence, or lack thereof, of a threshold ΔK for small cracks.

CONCLUSIONS

1. The acoustic scattering theory of Kino and Auld has been

verified in three different materials: Pyrex Glass, 7075-T651 aluminum, and quenched and tempered 4340 steel.

2. Acoustic predictions of crack depth agree with post-fracture measurements of crack depth with no more than 30% error for cracks which satisfy the long wavelength approximation. The average error was found to be 9%.
3. The estimated experimental uncertainty of each prediction of crack depth is in good agreement with measured errors between predicted and measured crack depth.
4. SAW reflection measurements of growing surface fatigue cracks provide in-situ feedback concerning crack size, stress intensity factor range, and crack opening behavior during fatigue cycling.
5. Combined SAW and SEM analyses of the opening behavior of small surface fatigue cracks are underway to investigate the relation between the crack closure stress and SAW saturation stress.

ACKNOWLEDGEMENT

The authors wish to thank the United States Department of Energy, Office of Basic Energy Sciences, Division of Materials Science and Engineering (Dr. S. Wolf) for supporting this research.

BIBLIOGRAPHY

1. Kino, G. S., "The Application of Reciprocity Theory to Scattering of Acoustic Waves by Flaws", JAP, 49, NO. 6, 3190-3199 (1978).
2. Auld, B. A., "General Electromechanical Reciprocity Relations Applied to the Calculation of Elastic Wave Scattering Coefficients", Wave Motion, 1, No. 1, 3-10 (1979).
3. Resch, M. T., Shyne, J. C. Kino, G. S. and Nelson, D. V., "Long Wavelength Rayleigh Wave Scattering from Microscopic Surface Fatigue Cracks", Proc. ARPA/AFML Rev. of Progress in Quantitative NDE, Boulder, CO (1981).
4. Resch, M. T., Nelson, D. V., Shyne, J. C. and Kino, G. S., "Acoustic Monitoring of Small Surface Fatigue Crack Growth", Advances in Crack Length Measurement, C. J. Beevers, ed., Engineering Materials Advisory Services Ltd., West Midlands, England (1983).

5. Resch, M. T., "Non-Destructive Evaluation of Small Surface Cracks Using Surface Acoustic Waves", Doctoral Dissertation, Stanford University, Stanford, CA (1982).
6. Resch, M. T., Khuri-Yakub, B. T., Kino, G. S. and Shyne, J. C., "The Acoustic Measurement of Stress Intensity Factors", Applied Physics Letters, 34, No. 3, 182-184 (1979).
7. Resch, M. T., Tien, J., Khuri-Yakub, B. T., Kino, G. S. and Shyne, J. C., "Acoustic Prediction of Fracture Stress", Mechanics of Nondestructive Testing, W.W. Stinchcombe, ed., Plenum Press, New York (1980).
8. Kline, S.J. and McClintock, F. A., "Describing Uncertainties in Single-Sample Experiments", Mechanical Engineering, January 1953.
9. Morris, W. L., "The Non-Continuum Crack Tip Deformation Behavior of Surface Microcracks", Met. Trans., 11A, 117-1123 (1980).
10. Morris, W. L., James, M. R. and Buck, O., "Growth Rate Models for Short Surface Cracks in Al 2219-T851", Met. Trans., 12A, 57-63 (1981).